



CHORUS

This is the accepted manuscript made available via CHORUS. The article has been published as:

Quantization of band tilting in modulated phononic crystals

H. Nassar, H. Chen, A. N. Norris, and G. L. Huang

Phys. Rev. B **97**, 014305 — Published 8 January 2018

DOI: [10.1103/PhysRevB.97.014305](https://doi.org/10.1103/PhysRevB.97.014305)

Quantization of band tilting in modulated phononic crystals

H. Nassar,¹ H. Chen,¹ A. N. Norris,² and G. L. Huang^{1,*}

¹*Department of Mechanical and Aerospace Engineering,
University of Missouri, Columbia, MO 65211, USA*

²*Department of Mechanical and Aerospace Engineering,
Rutgers University, Piscataway, NJ 08854-8058, USA*

A general theory of the tilting of dispersion bands in phononic crystals whose properties are being slowly and periodically modulated in space and time is established. The ratio of tilt to modulation speed is calculated, for the first time, in terms of Berry's phase and curvature and is proven to be a robust integer-valued Chern number. Derivations are based on a version of the adiabatic theorem for elastic waves demonstrated thanks to WKB asymptotics. Findings are exemplified in the case of a 3-periodic discrete spring-mass lattice. Tilted dispersion diagrams plotted using fully numerical simulations and semi-analytical calculations based on a numerically gauge invariant expression of Berry's phase show perfect agreement. One-way blocking of waves due to the tilt, and ultimately to the breaking of reciprocity, is illustrated numerically and shown to be highly significant across a limited number of unit cells suggesting the feasibility of experimental demonstrations. Finally, a version of the bulk-edge correspondence principle relating tilt of bulk bands to the number of one-way gapless edge states is demonstrated.

I. INTRODUCTION

The adiabatic theorem is a classical result of quantum mechanics.^{1,2} It applies to the Schrödinger equation and states that in an infinitely slow evolution of the Hamiltonian, a state, initially aligned with a given eigenstate, remains, at later times, in the same eigenstate and evolves solely by acquiring a phase factor. A careful analysis of the theorem carried by Berry³ led him to break the phase factor gained during the adiabatic evolution into two parts the second of which, later termed “Berry's phase”, turned out to be a concept with deep implications in solid state physics.⁴

It is perhaps only natural that the introduction of an adiabatic theorem for elastic waves was delayed so far. In comparison to electronic systems where changing the underlying potential is common practice using electric or magnetic fields (see, e.g., time-dependent perturbation theory and the working principle of lasers²), a change in the constitutive properties of an elastic medium such as its bulk modulus or mass density does not seem to be easily obtained and controlled. Recently, in conjunction with an increasing interest in breaking reciprocity and time-reversal symmetry, several techniques for dynamically changing the constitutive properties of an elastic medium have been identified. For instance, a giant and reversible light-induced softening was reported to occur in photo-sensitive network glasses⁵ suggesting a way of dynamically controlling their bulk modulus.⁶ Further, changing voltage boundary conditions and ambient magnetic fields were exploited to control the effective elastic properties in piezoelectric materials⁷⁻⁹ and magnetorheological elastomers,¹⁰ respectively. Other techniques are purely mechanical and trigger changes following a small-on-large scheme: large deformations applied to a non-linear medium effectively modify the underlying linearized properties for small overlay signals. Thus, changing the contact angles between cylinders confined in an array effectively alters the Young's

modulus of the array^{11,12} whereas shock waves guided in soft materials produce a moving front of high mass density.^{13,14}

When these changes are periodic in space and in time, the resulting medium is referred to as a modulated phononic crystal and displays interesting wave phenomena that have no counterpart in standard media.¹⁵⁻¹⁷ Of particular relevance to the present paper, is the demonstrated ability of a modulated phononic crystal to block and reflect waves if incident in a given direction while transmitting the same wave forms if incident in the opposite direction.^{6,18} As a matter of fact, the gaps of a modulated phononic crystal seem to be “tilted” with respect to their reference configuration in a non-modulated medium. This tilt breaks parity symmetry of the dispersion diagram and transforms a two-way gap into a couple of one-way gaps (Figure 1). Despite the existence of several case studies, a fundamental unifying theory characterizing tilts in a general context and with systematic tools is lacking. Such a theory, presented here, helps reveal salient features of tilts, robustness in particular, in a way that can guide future experimental and technological efforts.

The main purpose of the present paper is to characterize and quantify the modulation-induced tilt of dispersion bands. Specifically, we prove that the ratio of tilt to modulation speed is a robust topological quantized quantity: it does not depend on the detail of the space-time profiles of the constitutive parameters and only relies on a couple of well-defined qualitative properties. Indeed, from recent contributions,¹⁹⁻²¹ it can be inferred that said ratio is universally equal to 1 for a class of continuous phononic crystals and metamaterials whose properties depend on continuous space x and time t through the unique combination $x - Vt$ where V is the modulation speed. Here, by adapting the adiabatic theorem and the concept of Berry's phase to elasticity, a general theory of band tilting in arbitrarily modulated continuous or discrete media is

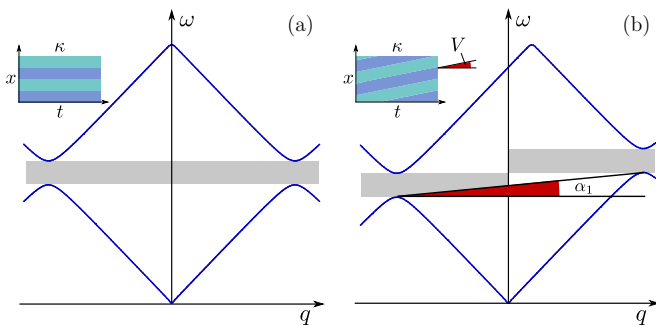


Figure 1. A space-time modulation of constitutive parameters (here, the bulk modulus κ) at speed V transforms a two-way bandgap (a) into two one-way bandgaps (b) by tilting the n th dispersion band by an angle α_n .

presented, provided that the modulation is slow.

II. THE ADIABATIC THEOREM FOR ELASTIC MEDIA

Consider the motion equation

$$\partial_t(M\partial_t u) = -Ku, \quad (1)$$

where, in the context of modulated phononic crystals, u is a displacement field and the mass and stiffness operators, respectively M and K , are both T -periodic functions of time. Stiffness K further depends on the Floquet-Bloch wavenumber q . Although relatively abstract, the above equation has the advantage of modeling elastic wave propagation in discrete as well as in continuous media. One way to see it is to notice that, regardless of the geometry of the underlying medium, by applying a proper discretization method, say the finite element method, we always end up with an equation of this form.

Associated to equation (1), is a set of (q, t) -dependent snapshot eigenstates (ω_n^2, Ψ_n) satisfying

$$\omega_n^2 M \Psi_n = K \Psi_n, \quad \langle \Psi_n, M, \Psi_m \rangle = \delta_{nm}, \quad (2)$$

with δ_{nm} being the Kronecker symbol and the brackets denoting the underlying Hermitian inner product. Then, for a given q , the adiabatic theorem states that the n th Floquet-Bloch eigenmode of equation (1) is

$$u(t) = \frac{1}{\sqrt{\omega_n(t)}} \exp \left[-i \int_0^t (\omega_n(s) + \dot{\gamma}_n(s)) ds \right] \Psi_n(t), \quad (3)$$

with Berry's connection $\dot{\gamma}_n$ given by

$$\dot{\gamma}_n = \text{Im} \langle \dot{\Psi}_n, M, \Psi_n \rangle, \quad (4)$$

provided that ω_n^2 remains a non-degenerate eigenvalue at all instants in time and that the modulation frequency $\nu = 2\pi/T$ is sufficiently small in the sense

$$\nu \ll \min_{m \neq n} |\omega_n - \omega_m|. \quad (5)$$

In particular, if the n th band is separated by gaps from bands $n \pm 1$ at $t = 0$, then it will remain so at all subsequent times. If not, scattering from one band to another will occur and will invalidate the theorem.^{19–21}

The proof of the foregoing result is based on WKB asymptotics and is detailed in appendix A. Inspecting equation (3), it is seen that a wave initially coinciding with the eigenmode $\Psi_n(0)$ remains at later times in the eigenmode $\Psi_n(t)$. It gains nonetheless two phase factors, one of which is the usual $\int_0^t \omega_n(s) ds$ that reduces to $\omega_n t$ in the absence of modulation, the other being at the origin of Berry's phase. Further, the transient wave changes its amplitude inversely proportionally to $\sqrt{\omega_n}$: the higher the frequency gets, the smaller the oscillations become.

Although not fundamentally new *per se*, the adiabatic theorem is included here as it cannot be found elsewhere for elastic waves. Similar results already exist in other physical contexts with an identical mathematical structure, e.g., the harmonic Schrödinger equation of a particle moving through a potential slowly varying in space.^{1,2,22}

III. TILT OF ELASTIC BANDS

The n th Floquet-Bloch eigenfrequency of the modulated medium, called Ω_n , can be extracted from (3) by factoring out all T -periodic quantities, leaving

$$\Omega_n = \frac{1}{T} \int_0^T \omega_n(t) dt + \frac{\gamma_n}{T}, \quad (6)$$

where

$$\gamma_n = \int_0^T \text{Im} \langle \Psi_n, M, \dot{\Psi}_n \rangle dt \quad (7)$$

is the elastic counterpart to the quantum mechanical Berry's phase. Thus, the n th eigenfrequency is averaged over a period and shifted by an amount equal to Berry's phase. Note that, representing an angle, Berry's phase is only well defined modulo 2π . Similarly, Ω_n is only well defined modulo the modulation frequency ν , an ambiguity predicted by Floquet-Bloch theorem. On the other hand, the phase factors $e^{i\gamma_n}$ and $e^{i\Omega_n T}$ are well defined and uniquely valued.

The tilting of dispersion bands caused by a slow modulation in a 1D periodic medium can now be quantified. Indeed, the tilt of the n th band is given by the ratio

$$\alpha_n \equiv \frac{\Omega_n(\pi/L) - \Omega_n(-\pi/L)}{2\pi/L} \quad (8)$$

where $\pm\pi/L$ denote the right and left end of the Brillouin zone respectively and L is the length of a unit cell. Given that ω_n is a periodic function of q , it has no effect on α_n , so that the tilt becomes

$$\alpha_n = V \frac{\gamma_n(\pi/L) - \gamma_n(-\pi/L)}{2\pi} \quad (9)$$

where $V \equiv L/T$ is the modulation speed.

Unlike Berry's phase, the tilt α_n represents a swept angle and admits thus a unique value. Said value of α_n can further be proven to be an integer multiple of the modulation speed V . As a matter of fact, both ends of the Brillouin zone correspond to the same physical configuration; hence, $\Omega_n(\pi/L)$ and $\Omega_n(-\pi/L)$ can only differ by an integer multiple of ν implying that α_n/V is an integer. This argument should not be abused however: since the two ends of the Brillouin zone are physically identical, one might be eager to conclude that the tilt vanishes systematically. But this is not necessarily the case in the same manner that $e^{ia} = e^{ib}$ does not necessitate $a = b$.

The quantization of α_n/V implies that this ratio is a robust topological quantity: continuous, small or large, perturbations in the underlying medium should induce continuous perturbations in α_n/V except that, being integer-valued, α_n/V cannot vary continuously other than by remaining constant. This holds as long as our working hypothesis of no degeneracies is respected. Conversely, a perturbation that leads to a change in α_n/V is one that cannot be completed while avoiding the appearance of degeneracies.

IV. NUMERICAL GAUGE INVARIANCE

Evaluating the shifted eigenfrequencies through (6) whether analytically or numerically is not a straightforward matter. Indeed, expression (4), based on which Ω_n is calculated, is only valid if the plugged-in Ψ_n is smooth with respect to t . Yet, determining a smooth single-valued expression for Ψ_n over $[0, T]$ can be troublesome.³ It is therefore of interest to find an alternative expression of Ω_n , and ultimately of Berry's phase, that can be evaluated with an arbitrary choice of Ψ_n , be it smooth or not with respect to t . Such expressions are qualified as "numerically gauge-invariant" in the sense that, even when discretized, they remain insensitive to the choice of Ψ_n . As such, numerically gauge-invariant expressions are well suited for numerical evaluation.

Thus, following a method attributed to Resta,²³ one is encouraged to re-write Berry's phase as the limit

$$\gamma_n = \lim_{N \rightarrow \infty} \arg \prod_r \langle \Psi_n(t^r), M(t^r), \Psi_n(t^{r+1}) \rangle, \quad (10)$$

where $\{t^r, r = 1 \dots N\}$ constitutes a discretization of $[0, T]$ with a step of the order of T/N ; see appendix B for a short proof. Remarkably, the evaluation of the above expression is insensitive to the smoothness of Ψ_n since substituting Ψ_n with $\Psi_n e^{i\beta}$, for arbitrary real-valued non-smooth β , produces no net effect.

For the same reasons, guided by the original work of Berry,³ the expression of the tilt is transformed into

$$\alpha_n = \frac{V}{2\pi} \iint_{\mathcal{T}} \mathcal{B}_n \, dq \, dt \quad (11)$$

where \mathcal{T} is the torus $[-\pi/L, \pi/L] \times [0, T]$ and

$$\mathcal{B}_n = 2 \operatorname{Im} \sum_{m \neq n} \frac{\langle \Psi_n, \partial_q K, \Psi_m \rangle \langle \Psi_m, \dot{K} - \frac{\omega_n^2 + \omega_m^2}{2} \dot{M}, \Psi_n \rangle}{(\omega_n^2 - \omega_m^2)^2} \quad (12)$$

is Berry's curvature. A derivation is detailed in appendix C. The above equation is a slight generalization to the one derived by Berry³ as it takes into account a non-identity parameter-dependent (here, time-dependent) mass operator. Further, as the integral of a Berry's curvature over a closed surface, the ratio α_n/V provides novel insight into how topological features described by a Chern number can manifest.^{4,24,25} When the crystal has a finite number of bands, the sum of Berry's curvature over all bands is zero, $\sum_n \mathcal{B}_n = 0$, implying the remarkable result that the sum of all tilts vanishes identically. In particular, in a discrete lattice, the sum of all tilts is systematically null. For crystals with an infinite number of bands, the sum need not vanish.¹⁹

Last, the expression of the tilt in terms of Berry's curvature allows to refine the result on robustness. For instance, assuming ω_n indefinitely approaches ω_{n+1} , tilts α_n and α_{n+1} are no longer well defined as \mathcal{B}_n and \mathcal{B}_{n+1} become singular and diverge. Nonetheless, $\mathcal{B}_n + \mathcal{B}_{n+1}$ remains non-singular. This generalizes immediately and implies that the sum of tilts $\sum_{m < k \leq n} \alpha_k/V$ of all bands between gaps number m and n is invariant and immune to perturbations as long as these gaps remain open even when intermediary gaps close.

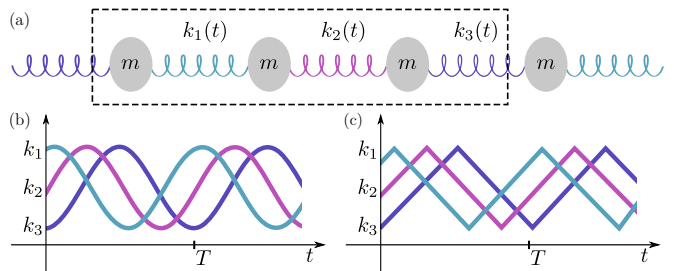


Figure 2. A modulated 3-periodic spring-mass lattice (a) and two examples of time profiles of its spring constants: sinusoidal (b) and triangular (c). A unit cell is framed in dashed lines.

V. EXAMPLE: 3-PERIODIC LATTICE

Consider the spring-mass lattice of Figure 2 whose unit cell contains three constant masses of values m_i connected through three springs of time-dependent T -periodic constants $k_i \equiv k_i(t)$, $i = 1, 2, 3$. Constancy of the masses is not required but is assumed for simplicity whereas the k_i are taken to be sine waves of the form

$$k_i(t) = k + \delta k \cos(\nu t + \theta_i), \quad \delta k > 0. \quad (13)$$

The governing motion equation then takes the form (1) where u is a 3×1 column vector of the displacements of

the masses within one unit cell and with

$$K = \begin{bmatrix} k_3 + k_1 & -k_1 & -k_3 Q^* \\ -k_1 & k_1 + k_2 & -k_2 \\ -k_3 Q & -k_2 & k_2 + k_3 \end{bmatrix}, \quad M = \begin{bmatrix} m_1 & 0 & 0 \\ 0 & m_2 & 0 \\ 0 & 0 & m_3 \end{bmatrix}. \quad (14)$$

Therein, $Q = e^{iq}$ is a phase factor function of the non-dimensional Floquet-Bloch wavenumber $q \in [-\pi, \pi]$.

The snapshot eigenstates (ω_n^2, Ψ_n) can be calculated by solving the now 3×3 eigenvalue problem (2) using standard numerical routines. Shifts and tilts were calculated through fully numerical transient simulations based on a space-time finite difference method^{19,20} as well as using the semi-analytical numerically gauge-invariant formulae (11) and (6) combined with (10). Results are plotted on Figure 3a and show perfect agreement. The parameters used are $m_1 = m_2 = m_3 = m = 1\text{g}$, $k = 5 \cdot 10^5\text{N/m}$, $\delta k = 0,5k$, $\omega^0 = \sqrt{k/m} = 22,3\text{kHz}$, $\nu = 0,1\omega^0$, $\theta_1 = \pi$, $\theta_2 = \pi/2$ and $\theta_3 = 0$. Due to the modulation-induced tilt, a directional bandgap is visible around the frequency ω^0 . Transient simulations of the waves emitted by a loading with a narrow band centered on that frequency reveal a significant left/right bias. The waterfall plots of Figure 4 show that emitted waves travel to the left almost exclusively.

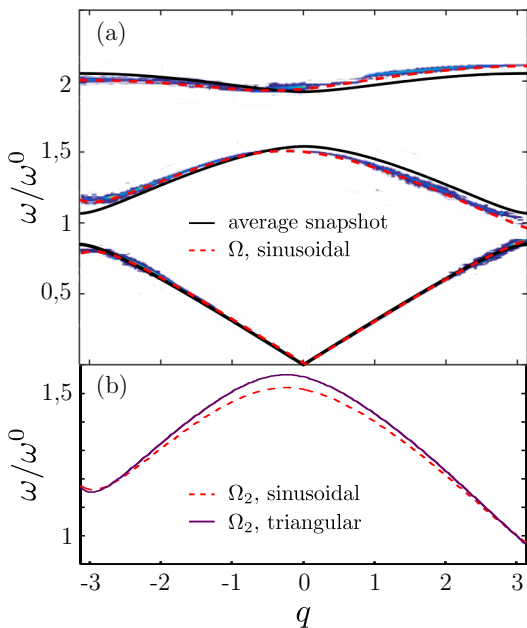


Figure 3. On (a): Dispersion diagrams of a 3-periodic sinusoidally modulated phononic crystal calculated numerically (blue level sets) and semi-analytically using Berry's phase (red dashed lines). Band tilting is visible in comparison to the average snapshot dispersion diagram (solid black lines). Floquet-Bloch replicas are dismissed for clarity. On (b): the second dispersion branch under a sinusoidal modulation (dashed line) compared to that under a triangular modulation (solid line). Although different, both bands feature the same tilt.

The array of tilts $(\alpha_1/V, \alpha_2/V, \alpha_3/V)$ realized in the above example is $(1, -2, 1)$. In fact, in a discrete medium,

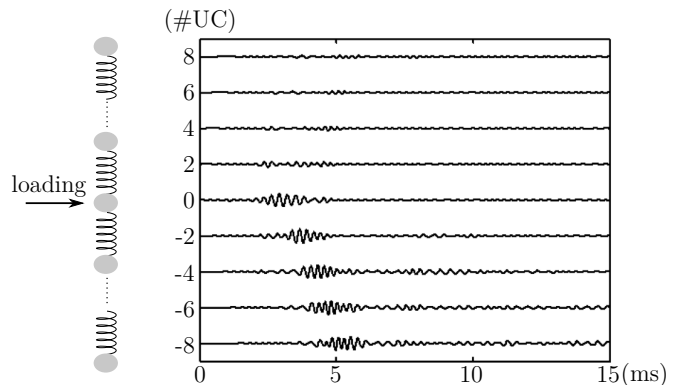


Figure 4. Waterfall plots of $u_1(t)$ in arbitrary units for every other unit cell, indexed with $\#UC$, generated by a narrow-band loading applied at the center of a sample composed of 81 unit cells.

for which the number of bands is finite and the sum of all tilts vanishes, it is impossible to impart the same non-zero tilt to all bands. In contrast, a uniform tilt in the dispersion diagram of a continuous medium can be obtained by modulating the constitutive parameters in a translation-like manner.¹⁹ That is, the spatial profile of a given constitutive parameter at any instant in time is identical to that at any other instant in time up to a spatial translation. A discrete medium cannot support such modulations.

Assuming a modulation of the form (13), only three arrays of tilts, namely $\pm(1, -2, 1)$ and $(0, 0, 0)$, are accessible depending on the relative values of the phase delays θ_i and masses m_i , $i = 1, 2, 3$; see Figure 5 for the corresponding phase diagrams. The array $(0, 0, 0)$ is also trivially accessible by suppressing the modulation. Other tilts cannot be obtained without modulating the masses as well. Diagrams 5a-b further illustrates the robustness of the tilt: being constant across large regions, the tilt is insensitive to uncertainty in the phase delays and in the values of the masses except near critical lines where phase transitions occur. This generalizes to other forms of uncertainty. For instance, changing the sinusoidal modulation into a triangular one (Figure 2b-c) leaving unchanged the other parameters perturbs the dispersion diagram but ultimately has zero influence on the tilts (Figure 3b).

VI. BULK-EDGE CORRESPONDENCE

Other than band tilting, non-zero Chern numbers suggest the existence of one-way edge modes in the space-frequency plane of (n, ω) according to the principle of bulk-edge correspondence.^{12,25,26} Hereafter, the principle is exemplified then proven.

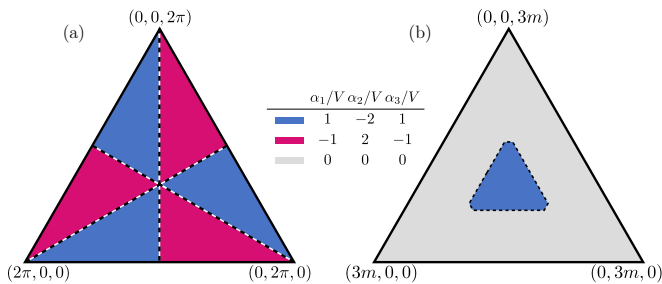


Figure 5. Phase diagrams of model (13) illustrating the array of tilts $(\alpha_1/V, \alpha_2/V, \alpha_3/V)$ as a function of phase delays $(\theta_1, \theta_2, \theta_3)$ on (a) and of masses (m_1, m_2, m_3) on (b) interpreted as barycentric coordinates in the planes $\{\theta_1 + \theta_2 + \theta_3 = 2\pi, m_1 = m_2 = m_3 = m\}$ and $\{m_1 + m_2 + m_3 = 3m, \theta_1 = 4\pi/3, \theta_2 = 2\pi/3, \theta_3 = 0\}$ respectively. Three arrays are accessible, $\pm(1, -2, 1)$ and $(0, 0, 0)$. Tilts are not defined over the dashed lines where degeneracies occur.

A. Example of bulk and edge snapshot spectra

Let us free a finite sample of the infinite 3-periodic modulated medium investigated above. Under free boundary conditions, snapshot eigenmode analysis reveals the existence of edge states within the bulk bandgaps at some instants in time; see Figure 6a. The evolution of a snapshot edge eigenmode goes through four states that constitute a periodic cycle illustrated on Figure 6b-e. Starting with state b which is localized at left edge, the frequency shifts down and state b transforms into state e. As the frequency decreases further into the first passing band, state e re-localizes in the bulk and then transforms into state d localized at the right edge. As the frequency increases now, state d transforms into state c which, by a similar mechanism, transforms into state b, and so on.

In the (n, ω) -space, the described cycle corresponds to a one-way edge state moving anti-clockwise; see Figure 6. Therein, the left and right boundaries correspond to the free boundaries of the sample whereas the top and bottom boundaries correspond to the boundaries of the first bulk bandgap. Note however that the cycle (b-e-d-c) does not represent the transient propagation of a physical signal; only (b-e) and (d-c) do. As a matter of fact, (b-e) and (d-c) transitions are adiabatic meaning that parameter t can be identified with real time and snapshot states are identical to transient states by the adiabatic theorem proven above. On the other hand, transitions (c-b) and (e-d) are not adiabatic since, according to Figure 6a, the gaps separating c and e from the passing bands become vanishingly small at which time these states will be scattered into bulk modes. In that case, parameter t no longer represents real time and snapshot states and transient states will differ significantly.

In any case, the number of edge states moving anti-clockwise in the first gap, called s_1^+ , is equal to $\alpha_1/V = 1$. As for the second gap, there is a unique edge state moving clockwise (not shown here): $s_2^- = 1$. Note also that $\alpha_1/V + \alpha_2/V = -1$. In general, letting s_n^\pm be the number

of robust edge states going anti-clockwise (respectively, clockwise) in gap number n , it will be proven that

$$s_n^+ - s_n^- = \frac{1}{V} \sum_{k \leq n} \alpha_k. \quad (15)$$

B. Number of robust edge states

Consider a bandgap hosting $\Delta s \equiv s_n^+ - s_n^-$ robust edge states and imagine a continuous perturbation closing all gaps except the one under consideration. Robustness means that such a perturbation does not change Δs . The resulting system has a unique gap separating two bulk bands. Although not necessary, it will be identified with a 2-periodic spring-mass lattice which should allow to gain deeper physical insight (Figure 7a). Number Δs can be counted by focusing on, say, the right edge of a finite sample. But edge modes decay exponentially so that, assuming the number of unit cells is large enough, the sample can be considered infinite to the left (Figure 7b). As for the boundary condition, it does not influence Δs by robustness. Thus, without loss of generality, the boundary is fixed.

Calling $m_{1,2}$ and $k_{1,2}$ the masses and spring constants within one unit cell, it is easy to check that a unique edge mode exists when $m_1 = m_2$ and $k_1 < k_2$. Further, it has an eigenvalue $\omega^2 = (k_1 + k_2)/m_2$ and makes masses m_2 oscillate while all masses m_1 remain at rest (Figure 7b). As m_2 is infinitesimally perturbed upwards, frequency decays implying that the edge mode is going clockwise whereas if m_2 is perturbed downwards, frequency increases implying that the edge mode is going anti-clockwise. In conclusion, counting the number of times m_2 decreases below m_1 while k_1 is smaller than k_2 , denoted $N(m_2 \downarrow m_1, k_1 < k_2)$, and the number of times m_2 increases above m_1 while k_1 is smaller than k_2 , denoted $N(m_2 \uparrow m_1, k_1 < k_2)$, one has

$$\Delta s = N(m_2 \downarrow m_1, k_1 < k_2) - N(m_2 \uparrow m_1, k_1 < k_2). \quad (16)$$

See Figure 7a for an illustration. Next, the tilt of the acoustic branch is calculated and proven to admit the same expression as Δs .

C. Tilt in a 2-band system

The foregoing 2-band model can be described by the stiffness and mass matrices

$$K = \begin{bmatrix} k_1 + k_2 & -k_1 - k_2 Q^* \\ -k_1 - k_2 Q & k_1 + k_2 \end{bmatrix}, \quad M = \begin{bmatrix} m_1 & 0 \\ 0 & m_2 \end{bmatrix}. \quad (17)$$

Recall that $m_{1,2}$ and $k_{1,2}$ are T -periodic functions of time such that the gap never closes. That is, $k_1 = k_2$ and $m_1 = m_2$ never occur simultaneously. By a change of basis, $\Psi \mapsto \sqrt{M}\Psi$, it is possible to rewrite the stiffness

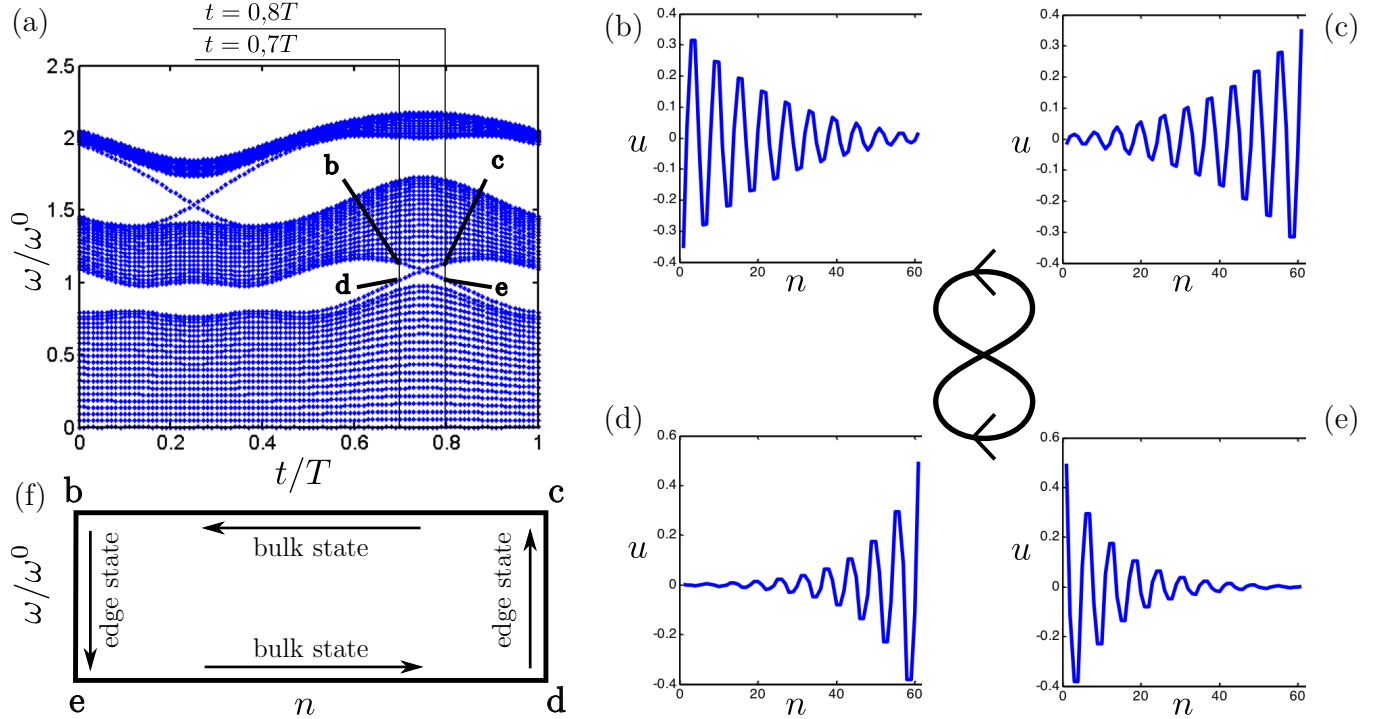


Figure 6. (a): Snapshot normalized eigenfrequencies of a finite slab of a 3-periodic modulated medium composed of 60 masses under free boundary conditions. Two bandgaps are visible and are traversed by the eigenfrequencies of edge states. The edge states within the first gap at $t = 0,7T$ and $t = 0,8T$ are labeled b-e and their spatial profiles are plotted in (b-e), respectively, where n is the mass index and u is displacement in arbitrary units. The oriented loop indicates the order in which the states appear with time. (f): the cycle (b-e-d-c) illustrated as a one-way edge state in (n, ω) -space.

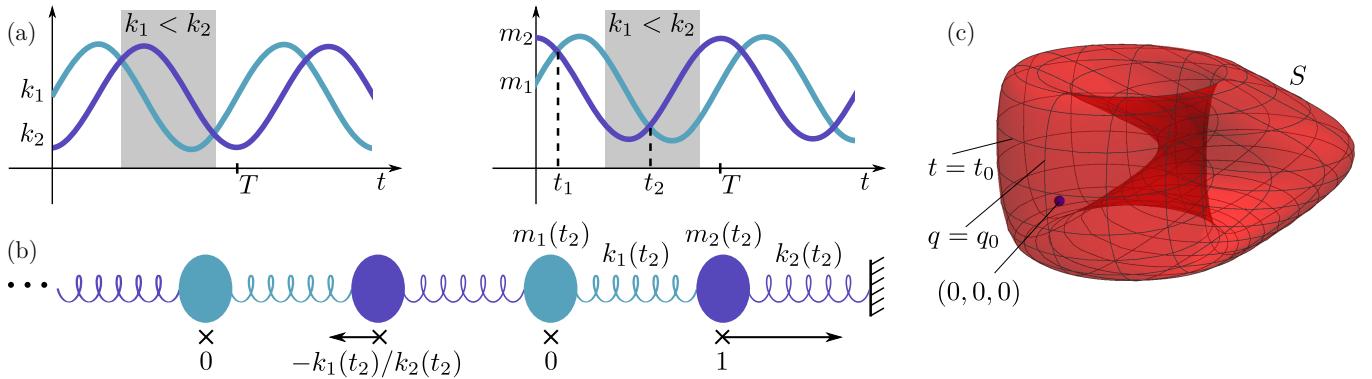


Figure 7. Bulk-edge correspondence: (a) an example of a periodic modulation in a 2-band system. In the region $k_1 < k_2$, m_2 crosses m_1 one time while increasing and zero time while decreasing so that $N(m_2 \uparrow m_1, k_1 < k_2) = 1$, $N(m_2 \downarrow m_1, k_1 < k_2) = 0$ and $\Delta s = -1$. (b) A semi-infinite sample with fixed boundary: an edge mode appears at $t = t_2$ for which $m_1 = m_2$ and $k_1 < k_2$. Arrows and assigned values correspond to normalized displacement magnitudes and show that every other mass is at rest. The decay rate is $\log(k_1/k_2)$ and the frequency is $\sqrt{(k_1 + k_2)/m_2}$. As m_2 is increasing at t_2 , the frequency of the edge mode is decreasing. (c) The corresponding surface $S : (q, t) \mapsto (X, Y, Z)$: S wraps once around the origin covering a solid angle of -4π due to its orientation meaning that $\alpha/V = -1$.

and mass matrices as

$$K = \begin{bmatrix} W + Z & X - iY \\ X + iY & W - Z \end{bmatrix}, \quad M = \begin{bmatrix} 1 & 0 \\ 0 & 1 \end{bmatrix}, \quad (18)$$

with

$$W = \frac{k_1 + k_2}{2} \left(\frac{1}{m_1} + \frac{1}{m_2} \right), \quad X = \frac{-k_1 - k_2 \cos q}{\sqrt{m_1 m_2}},$$

$$Y = \frac{k_2 \sin q}{\sqrt{m_1 m_2}}, \quad Z = \frac{k_1 + k_2}{2} \left(\frac{1}{m_1} - \frac{1}{m_2} \right).$$

Note that parameter W has no influence on the shape of the eigenmodes and can be dropped with no loss of generality. With these notations, thanks to the result of Berry,³ the tilt of the acoustic branch α is equal to $V/4\pi$ times the solid angle of the surface $S : (q, t) \mapsto (X, Y, Z)$ as seen from $(0, 0, 0)$ in the (X, Y, Z) -space; see Figure 7c. In other words, $\alpha/V = N$ the number of times that S wraps around the origin. Surface S being closed, α/V is quantized as expected and is invariant upon re-scaling (X, Y, Z) into

$$X = -\frac{k_1}{k_2} - \cos q, \quad Y = \sin q, \quad Z = \frac{m_2}{m_1} - 1. \quad (19)$$

A cross section $t = t_0$ of S is therefore a circle in a plane $Z = Z_0$ of center $(-k_1/k_2, 0)$, radius 1 and traversed clockwise. Thus, it wraps around the origin once each time Z crosses 0 (or m_1 crosses m_2) while $k_1 < k_2$. Counting these occurrences lead to the expression

$$\alpha/V = N(m_2 \downarrow m_1, k_1 < k_2) - N(m_2 \uparrow m_1, k_1 < k_2). \quad (20)$$

That is, $\alpha/V = \Delta s$.

In order to conclude, the perturbation reducing the original system to a 2-band system is undone. Meanwhile, the sum of all tilts below gap number n remains invariant so that $\alpha/V = \sum_{k \leq n} \alpha_k/V$. This ends the proof of the bulk-edge correspondence principle (15).

VII. CONCLUSION

The presented theory succeeds in providing three consistent analytical expressions for the tilt in the dispersion diagram of a modulated phononic crystal given the set of its snapshot dispersion diagrams; the first as a Berry's phase, the second as a Chern number and the third as the number of one-way edge states. Band tilting accompanied by non-reciprocal phenomena appears then as a novel consequence to bulk band topology. Proven robustness as well as the parameters used in the simulations and the limited number of unit cells necessary for the observation of the tilt-induced left/right radiation bias all lead us to believe that an experimental demonstration of the phenomenon should be within reach. Note last that topological aspects, although qualitatively insightful, do not provide quantitative estimates of the magnitude of the radiation bias and further theoretical efforts dealing with this issue are still needed.

ACKNOWLEDGMENTS

This work is supported by the Air Force Office of Scientific Research under Grant No. AF 9550-15-1-0016 with Program Manager Dr. Byung-Lip (Les) Lee and the NSF EFRI under award No. 1641078.

Appendix A: WKB asymptotics

The motion equation in a linearly elastic solid takes the form

$$\partial_t(\rho \partial_t u) = \nabla \cdot (C : \nabla^s u). \quad (A1)$$

Assuming spatial periodicity, applying the Floquet-Bloch transformation yields

$$\partial_t(\rho \partial_t u) = (\nabla + iq) \cdot \{C : [(\nabla + iq) \otimes u]\} \quad (A2)$$

which can be put in the more condensed form (1). Given that equation (1) holds as well for a discrete structure, it will be taken as the starting point of the subsequent derivations which are therefore valid for both continuous and discrete phononic crystals.

First, recall that equation (1) admits a set of snapshot eigenstates satisfying equation (2) so that the identity

$$\langle \partial_t \Psi_n, M, \Psi_m \rangle + \langle \Psi_n, \partial_t M, \Psi_m \rangle + \langle \Psi_n, M, \partial_t \Psi_m \rangle = 0 \quad (A3)$$

holds by differentiation with respect to time.

Then, the motion equation is scaled into

$$\partial_t(M(\epsilon t) \partial_t u^\epsilon(t)) = -K(\epsilon t) u^\epsilon(t) \quad (A4)$$

where focus is on the limit $\epsilon \rightarrow 0$ corresponding to an infinitely slow evolution. Alternatively, upon the change of variables $t \rightarrow t/\epsilon$, the above equation transforms into

$$\epsilon^2 \partial_t(M(t) \partial_t u^\epsilon(t)) = -K(t) u^\epsilon(t). \quad (A5)$$

The WKB ansatz

$$u^\epsilon = A^\epsilon e^{-i\phi/\epsilon}, \quad A^\epsilon = A + \epsilon \delta A + \dots \quad (A6)$$

is known to be suitable for this type of equations and is used hereafter.²² In the new variables A^ϵ and ϕ , the motion equation becomes

$$KA^\epsilon = -\epsilon^2 \left[\dot{M} \left(\dot{A}^\epsilon - i\dot{\phi} A^\epsilon / \epsilon \right) + M \left(\ddot{A}^\epsilon - 2i\dot{\phi} \dot{A}^\epsilon / \epsilon - (\dot{\phi})^2 A^\epsilon / \epsilon^2 - i\ddot{\phi} A^\epsilon / \epsilon \right) \right] \quad (A7)$$

where ∂_t is denoted as a superimposed dot to simplify reading. Substituting (A6) into (A5) and keeping the leading order terms entail

$$KA = (\dot{\phi})^2 MA. \quad (A8)$$

Thus, $((\dot{\phi})^2, A)$ is a snapshot eigenstate (ω_n^2, Ψ_n) for some n :

$$A \equiv A_n(t) \equiv a_n(t) \Psi_n(t), \quad \dot{\phi} \equiv \dot{\phi}_n(t) = \pm \omega_n(t). \quad (A9)$$

Choosing $\phi(0) = 0$ with no loss of generality, we obtain by integration

$$\phi \equiv \phi_n(t) = \pm \int_0^t \omega_n(t) dt. \quad (A10)$$

Keeping first order terms then gives

$$-\sum_{\dot{\phi}_m=\dot{\phi}_n} K\delta A_m = \sum_{\dot{\phi}_m=\dot{\phi}_n} \dot{M} \left(-i\dot{\phi}_m A_m \right) + M \left(-2i\dot{\phi}_m \dot{A}_m - (\dot{\phi}_m)^2 \delta A_m - i\ddot{\phi}_m A_m \right) \quad (\text{A11})$$

where the summation is carried over all indices m yielding the same eigenvalue $\dot{\phi}_n$. When an eigenvalue is non-degenerate, the sum contains a single term. Projecting onto the eigenvectors Ψ_m , we obtain

$$\dot{a}_n = -\frac{\ddot{\phi}_n}{2\dot{\phi}_n} a_n + \sum_{\dot{\phi}_m=\dot{\phi}_n} \frac{\langle \dot{\Psi}_n, M, \Psi_m \rangle - \langle \Psi_n, M, \dot{\Psi}_m \rangle}{2} a_m \quad (\text{A12})$$

where we have used (A3) to get rid of terms containing \dot{M} . We need to point out here that in addition to the hypothesis of slow evolution, a second implicit hypothesis is involved in the foregoing derivation; that is that the multiplicity of each eigenvalue is constant during the whole evolution. We thus exclude crossings between eigenvalues: a situation where $\omega_n(t_0) \neq \omega_m(t_0)$ and $\omega_n(t_1) = \omega_m(t_1)$ is precluded.

Consider now a non-degenerate eigenvalue ω_n ; that is an eigenvalue that remains simple during the whole evolution. Relation (A12) specifies into

$$\dot{a}_n = -\frac{\ddot{\phi}_n}{2\dot{\phi}_n} a_n + \frac{\langle \dot{\Psi}_n, M, \Psi_n \rangle - \langle \Psi_n, M, \dot{\Psi}_n \rangle}{2} a_n \quad (\text{A13})$$

and can be integrated yielding

$$a_n(t) = a_n(0) \sqrt{\frac{|\dot{\phi}_n(0)|}{|\dot{\phi}_n(t)|}} \exp \left(-i \int_0^t \dot{\gamma}_n(s) ds \right) \quad (\text{A14})$$

with $\dot{\gamma}_n$ given by (4)

Combining the foregoing results and dropping ϵ , the solution u can be expressed, to leading order, according to (3) concluding thus the proof of the adiabatic theorem.

Appendix B: Resta's formula for Berry's phase

Following Resta,²³ consider a discrete set of instants in time t^r covering $[0, T]$, say $t^r = rT/N$, $r = 1 \dots N$. The increment in Berry's phase between t^r and t^{r+1} is given by (4) and reads

$$\delta_r^{r+1} \gamma_n = \text{Im} \langle \Psi_n(t^r), M(t^r), \Psi_n(t^{r+1}) - \Psi_n(t^r) \rangle. \quad (\text{B1})$$

Given that $\langle \Psi_n(t^r), M(t^r), \Psi_n(t^r) \rangle = 1$ is real, this becomes

$$\delta_r^{r+1} \gamma_n = \text{Im} \langle \Psi_n(t^r), M(t^r), \Psi_n(t^{r+1}) \rangle \quad (\text{B2})$$

which is further equal to

$$\delta_r^{r+1} \gamma_n = \frac{\text{Im} \langle \Psi_n(t^r), M(t^r), \Psi_n(t^{r+1}) \rangle}{|\langle \Psi_n(t^r), M(t^r), \Psi_n(t^{r+1}) \rangle|} \quad (\text{B3})$$

to first order in T/N . The above ratio can be alternatively written as

$$\delta_r^{r+1} \gamma_n = \arg \langle \Psi_n(t^r), M(t^r), \Psi_n(t^{r+1}) \rangle. \quad (\text{B4})$$

Summing, it comes that

$$\gamma_n = \sum_r \delta_r^{r+1} \gamma_n = \sum_r \arg \langle \Psi_n(t^r), M(t^r), \Psi_n(t^{r+1}) \rangle, \quad (\text{B5})$$

which, in a product form and making explicit the underlying limit, is equivalent to equation (10).

Appendix C: Berry's curvature

Following the original work of Berry,³ let us denote

$$\mathcal{A}_n^t = \dot{\gamma}_n = \text{Im} \langle \Psi_n, M, \dot{\Psi}_n \rangle. \quad (\text{C1})$$

Similarly, for reasons that will soon become clear, we define

$$\mathcal{A}_n^q = \text{Im} \langle \Psi_n, M, \partial_q \Psi_n \rangle. \quad (\text{C2})$$

Together, $(\mathcal{A}_n^q, \mathcal{A}_n^t)$ form a vector called Berry's connection. The tilt then takes the form of a path integral

$$\alpha_n = V \frac{\gamma_n(\pi/L) - \gamma_n(-\pi/L)}{2\pi} = \frac{V}{2\pi} \oint_{\mathcal{C}} \mathcal{A}_n^q dq + \mathcal{A}_n^t dt \quad (\text{C3})$$

where \mathcal{C} is the oriented loop $\{\pi/L\} \times [0, T] \cup \{-\pi/L\} \times [T, 0]$ in the (q, t) -space (Figure 8). Since \mathcal{C} is also the boundary of the torus $\mathcal{T} = [-\pi/L, \pi/L] \times [0, T]$, Stokes theorem yields

$$\alpha_n = \frac{V}{2\pi} \iint_{\mathcal{T}} (\partial_q \mathcal{A}_n^t - \partial_t \mathcal{A}_n^q) dq dt \equiv \frac{V}{2\pi} \iint_{\mathcal{T}} \mathcal{B}_n dq dt \quad (\text{C4})$$

where \mathcal{B}_n is Berry's curvature. Next, we derive an explicit formula for \mathcal{B}_n .

First, using the chain rule and that $\partial_q M = 0$, write \mathcal{B}_n as

$$\mathcal{B}_n = 2 \text{Im} \left\{ \langle \partial_q \Psi_n, M, \dot{\Psi}_n \rangle - \frac{\langle \Psi_n, \dot{M}, \partial_q \Psi_n \rangle}{2} \right\}. \quad (\text{C5})$$

Then, expanding along the orthogonal eigenstates Ψ_m , we obtain

$$\mathcal{B}_n = \sum_m 2 \text{Im} \left\{ \langle \partial_q \Psi_n, M, \Psi_m \rangle \langle \Psi_m, M, \dot{\Psi}_n \rangle - \langle \Psi_n, \dot{M}, \Psi_m \rangle \langle \Psi_m, M, \partial_q \Psi_n \rangle / 2 \right\}. \quad (\text{C6})$$

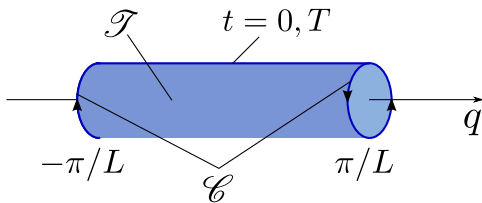


Figure 8. Stokes theorem: an integral over boundary \mathcal{C} can be transformed into an integral over domain \mathcal{T} . Since $t = 0, T$ and $q = \pm\pi/L$ are physically identical, domain \mathcal{T} can be identified with a torus. Path \mathcal{C} is then the boundary of torus \mathcal{T} cut open along $q = \pm\pi/L$.

The terms with $m = n$ can be omitted since they have no imaginary part.

Now we calculate the term $\langle \Psi_m, M, \dot{\Psi}_n \rangle$. Starting

with equation (2), applying ∂_t yields

$$-2\omega_n \dot{\omega}_n M \Psi_n - \omega_n^2 \dot{M} \Psi_n - \omega_n^2 M \dot{\Psi}_n = -\dot{K} \Psi_n - K \dot{\Psi}_n. \quad (\text{C7})$$

Projecting onto Ψ_m , we obtain

$$\begin{aligned} \langle \Psi_m, M, \dot{\Psi}_n \rangle &= \frac{\langle \Psi_m, \dot{K}, \Psi_n \rangle}{\omega_n^2 - \omega_m^2} \\ &\quad - \frac{\omega_n^2}{\omega_n^2 - \omega_m^2} \langle \Psi_m, \dot{M}, \Psi_n \rangle. \end{aligned} \quad (\text{C8})$$

In the same manner, applying ∂_q and projecting, we see that

$$\langle \Psi_m, M, \partial_q \Psi_n \rangle = \frac{\langle \Psi_m, \partial_q K, \Psi_n \rangle}{\omega_n^2 - \omega_m^2}. \quad (\text{C9})$$

Substituting these relations into the expression of \mathcal{B}_n , we conclude that Berry's curvature admits expression (12).

-
- * Corresponding author: huangg@missouri.edu
- ¹ J. Sakurai, *Modern quantum mechanics*, edited by S. Tuan (Addison-Wesley, Reading, Massachusetts, 1994).
 - ² D. J. Griffiths, *Introduction to quantum mechanics*, second ed. (Pearson Prentice Hall, 2004).
 - ³ M. V. Berry, Proc. R. Soc. A **392**, 45 (1984).
 - ⁴ D. Xiao, M. C. Chang, and Q. Niu, Rev. Mod. Phys. **82**, 1959 (2010).
 - ⁵ J. Gump, I. Finkler, H. Xia, R. Sooryakumar, W. J. Bresser, and P. Boolchand, Phys. Rev. Lett. **92**, 245501 (2004).
 - ⁶ N. Swinck, S. Matsuo, K. Runge, J. O. Vasseur, P. Lucas, and P. A. Deymier, J. Appl. Phys. **118**, 063103 (2015).
 - ⁷ F. Casadei, T. Delperio, A. Bergamini, P. Ermanni, and M. Ruzzene, J. Appl. Phys. **112**, 064902 (2012).
 - ⁸ Y. Y. Chen, R. Zhu, M. V. Barnhart, and G. L. Huang, Sci. Rep. **6**, 35048 (2016).
 - ⁹ Y. Y. Chen, G. L. Huang, and C. T. Sun, J. Vib. Acoust. **136**, 061008 (2014).
 - ¹⁰ K. Danas, S. V. Kankanala, and N. Triantafyllidis, J. Mech. Phys. Solids **60**, 120 (2012).
 - ¹¹ F. Li, C. Chong, J. Yang, P. G. Kevrekidis, and C. Daraio, Phys. Rev. E - Stat. Nonlinear, Soft Matter Phys. **90**, 053201 (2014).
 - ¹² R. Chaunsali, F. Li, and J. Yang, Sci. Rep. **6**, 30662 (2016).
 - ¹³ E. J. Reed, M. Soljačić, and J. D. Joannopoulos, Phys. Rev. Lett. **91**, 133901 (2003).
 - ¹⁴ E. J. Reed, M. Soljačić, M. Ibanescu, and J. D. Joannopoulos, J. Comput. Mater. Des. **12**, 1 (2005).
 - ¹⁵ K. A. Lurie, Int. J. Solids Struct. **34**, 1633 (1997).
 - ¹⁶ K. A. Lurie, *An introduction to the mathematical theory of dynamic materials* (Springer, New York, NY, 2007).
 - ¹⁷ G. W. Milton and O. Mattei, Proc. R. Soc. A **473**, 20160819 (2017).
 - ¹⁸ G. Trainiti and M. Ruzzene, New J. Phys. **18**, 083047 (2016).
 - ¹⁹ H. Nassar, X. C. Xu, A. N. Norris, and G. L. Huang, J. Mech. Phys. Solids **101**, 10 (2017).
 - ²⁰ H. Nassar, H. Chen, A. N. Norris, M. R. Haberman, and G. L. Huang, Proc. R. Soc. A **473**, 20170188 (2017).
 - ²¹ H. Nassar, H. Chen, A. N. Norris, and G. L. Huang, Extrem. Mech. Lett. **15**, 97 (2017).
 - ²² C. M. Bender and S. A. Orszag, *Advanced mathematical methods for scientists and engineers I: Asymptotic methods and perturbation theory* (Springer-Verlag New York, 1999).
 - ²³ R. Resta, Rev. Mod. Phys. **66**, 899 (1994).
 - ²⁴ D. J. Thouless, M. Kohmoto, M. P. Nightingale, and M. den Nijs, Phys. Rev. Lett. **49**, 405 (1982).
 - ²⁵ D. J. Thouless, Phys. Rev. B **27**, 6083 (1983).
 - ²⁶ J. K. Asbóth, L. Oroszlány, and A. Pályi, *A short course on topological insulators: Band structure and edge states in one and two dimensions* (Springer International Publishing, 2016).
 - ²⁷ Y. Hatsugai and T. Fukui, Phys. Rev. B **94**, 041102 (2016).